Lumped-Parameter Model and Nonlinear DSSI Analysis

Maotian Luan

Dalian University of Technology, Dalian, China

Gao Lin

Dalian University of Technology, Dalian, China

W. F. Chen

Purdue University, West Lafayette, Indiana

Proceedings: Third International Conference on Recent Advances in Geotechnical Earthquake Engineering and Soil Dynamics, April 2-7, 1995, Volume I, St. Louis, Missouri

Lumped-Parameter Model and Nonlinear DSSI Analysis

Paper No. 5.02

Maotian Luan and Gao Lin
Professors of Civil Engineering, Dalian University of Technology, Dalian, P.R. China

W.F. Chen
George Goodwin Distinguished Professor, Head of Structural Engineering, School of Civil Engineering, Purdue University, West Lafayette, Indiana

SYNOPSIS A 2-degrees-of-freedom discrete model with 8 constant lumped parameters is developed to equivalently simulate frequency-dependent dynamic impedances of the elastic halfspace. The equations of motion for the nonlinear dynamic soil-structure interaction (DSSI) analysis are established in the time domain and then nonlinear seismic responses of the coupling system are predicted by the proposed iterative procedure. Based on numerical results for three typical shear-type structures, effects of the shear stiffness of underlying soils and different ground motions on dynamic responses are examined.

INTRODUCTION

The dynamic behavior of the structures founded on soft or weak subsoils under strong earthquake shaking is obviously different from that of the same structures supported on firm foundation soils. As usual, the earthquake-induced loading exerting on the superstructure estimated on the basis of rigid foundation assumption cannot authentically match actual performance. It is recognized that the dynamic soil-structure interaction (DSSI) effect on the structural seismic response cannot be overlooked. On the one hand, structural vibration will influence both peak amplitude and spatial distribution of ground motion propagating into underlying foundation soils which will be obviously different with free-field performance. On the other hand, structural dynamic response characteristics will varied due to the soil flexibility. In comparison with rigid base condition, the fundamental period of the coupling system will be increased to a certain extent. In addition, a portion of vibrating energy of the building will be dissipated by both the radiation damping due to waves out-going to far field soils and the hysteresis damping of vibrating soil materials, both of energy dissipative mechanisms do not exist for the structure built on solid ground surface. The main issue in the soil-structure interaction analysis is to evaluate the dynamic impedance functions of foundation soils on the structural footing which is of frequency-dependent nature. Frequency-domain formulations for solving seismic response of the coupling systems gained popular usages, but mostly based on the assumption of linear elastic behavior of structural members and soil materials in common practice. However, most real structures behave nonlinearly, particularly for levels of response that correspond to structural damage. Such behavior may be caused by nonlinear constitutive laws of constituent materials or by the transient sliding or local debonding of interfaces between structure footing and foundation soils. While these factors are considered in the earthquake-resistant design of structures, a rational nonlinear computational method for the coupled structure-footing-foundation system should be worked out directly in the time domain. This problem still keeps challenging in the field of earthquake engineering.

In this paper, a discrete model with 8 lumped parameters is proposed to simulate the frequency-dependent dynamic impedance of linear elastic halfspace. The equations of motion for nonlinear analysis of dynamic soil-structure interaction system are formulated in the time domain and then numerical computations for typical cases are performed to display effects of subsoil rigidity, ground motion characteristics on structural nonlinear seismic responses.

LUMPED-PARAMETER MODEL FOR SOIL DYNAMIC IMPEDANCE

The dynamic impedance is a basic issue in soil-structure interaction analyses. Many researchers have made their efforts to develop analytical or numerical methods or simplified approximations (Gazetas 1983). Up till present, the theory of (visco-) elastic half-space with a massless disk is frequently applied to describe the dynamic impedance of foundation soils. The real and imaginary parts correspond respectively to dynamic spring and radiation damping coefficients of soil reactions. Because of their dependency on excited frequency, these functions can be directly used only in the frequency domain. Hence such an analysis is effective only in the linear case. For nonlinear structures, however, the dynamic analysis must be performed in the time domain. Therefore, it is necessary to reproduce the dynamic impedance function by using a lumped-parameter system consisting of a series of simple mechanical elements such as mass, dashpot and spring in a certain manner based on the Winkler-like concept. The key problem for such types of discrete models is to select the appropriate values of relevant equivalent parameters. In the beginning, the simplest SDOF model is commonly established (see Gazetas 1983; Ghaffar-Zadeh and Chapel 1983). Unfortunately, this type of models have several drawbacks as pointed out by Jean, Lin and Penzien (1990). In order to overcome these deficiencies, Wolf and Somaini (1986) developed a 2-DOF discrete model with 5 constant lumped parameters to represent the unbounded half-space soils. Alternatively, De Barros and Luco (1990) presented another 5-parameters mechanical model involving a combination of two-springs, two-dampers and a mass. Furthermore, based on the compliance functions obtained by Luco and Westmann (1973), Jean et al (1990) proposed discrete models with 3 DOFs for different vibration modes of footing, in which 10 or 18 frequency-independent parameters are determined by the least square method. These investigations have shown that a vibrating system with 2 or 3 DOFs for dynamic impedance modelling will receive a fair reasonable accuracy with the least computational efforts.

Here, a discrete mechanical model with 2-DOFs and 8 frequency-independent lumped parameters is proposed to equivalently replace the uniform elastic half-space, as depicted in Fig.1. The force-displacement relation for harmonic sway or rocking vibration of this system is established for reproducing the dynamic impedances of a rigid massless footing supported on an uniform elastic half-space. The values of the dimensionless model parameters k^*_{f1}, k^*_{f2}, k^*_{f3}, c^*_{f1}, c^*_{f2}, c^*_{f3}, m^*_{f1} and m^*_{f2} are obtained by fitting the functions of real and imaginary parts given by the force-displacement relation of this simple mechanical model to the corresponding functions calculated from the solution of the dynamic mixed boundary-value problem of a rigid foundation attached to an elastic half-space. Optimization techniques are employed to minimize the square of weighted residuals of these two functions. The variations of dynamic impedance functions for horizontal and rocking vibration modes with dimensionless excited frequency $a_0 = r_0\omega/V_s$ computed by Veletsos and Wei (1971) are taken as the exact target solutions as given in Fig.2 and Fig.3 for the Poisson's ratio values of 0, 1/3, 1/2. From these figures it can be seen that the proposed discrete model can rather well match both real and imaginary parts of the dynamic impedances over a wide frequency range. Listed in Table 1 are the corresponding equivalent parameters achieved by optimization. Here as usual, the coupling effect between sway and rocking vibrations is neglected.

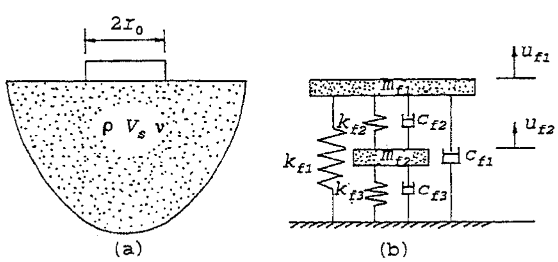

Fig.1. 8-Lumped Parameter Model Representation for Dynamic Impedance of Foundation Soil

TABLE 1. Optimized Values of Lumped Parameters of Discrete Models for Soil Impedances

	ν	m^*_{f1}	m^*_{f2}	k^*_{f1}	k^*_{f2}	k^*_{f3}	c^*_{f1}	c^*_{f2}	c^*_{f3}
	0	0.0006	0.211	2.118	-0.504	0.919	1.181	-0.426	1.069
Sway	1/3	0.0013	0.347	2.085	-0.447	0.761	1.149	-0.509	1.194
Mode	0.45	-0.0016	0.338	2.166	-0.471	0.790	1.125	-0.511	1.175
	1/2	-0.0035	0.340	2.158	-0.469	0.789	1.126	-0.512	1.178
	0	-0.0049	0.226	1.882	-0.376	0.656	0.972	-0.526	1.079
Rocking	1/3	-0.0016	0.229	1.864	-0.388	0.704	0.937	-0.519	1.116
Mode	0.45	0.0166	0.237	1.856	-0.376	0.672	0.868	-0.494	1.063
	1/2	0.0294	0.218	1.839	-0.444	0.941	0.722	-0.398	0.963

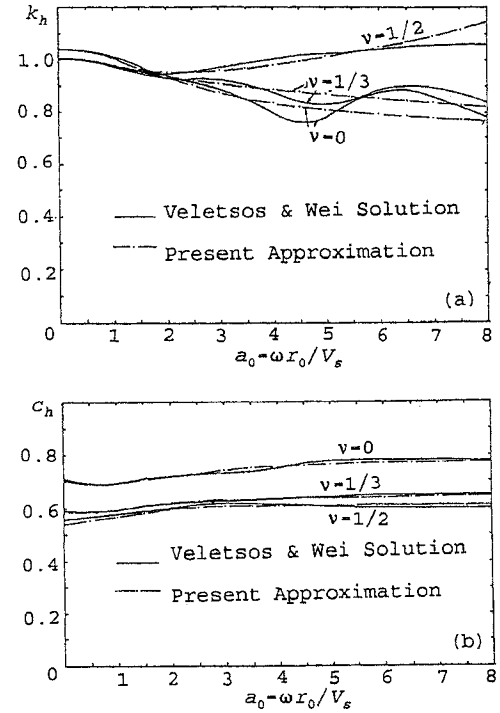

Fig.2. Comparisons of Sway Impedances

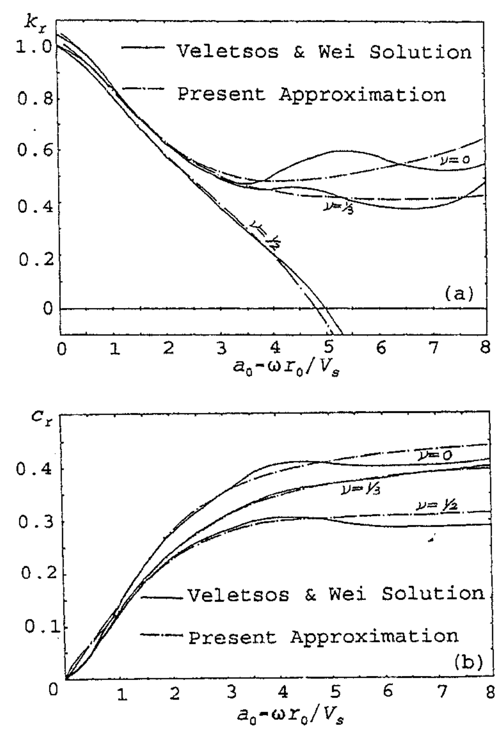

Fig.3. Comparisons of Rocking Impedances

Considering the dynamic equilibrium condition and deformation compatibility of the discrete system shown in Fig.1(b) leads to the resulting forces induced by the inertial effect of masses and interaction effect between footing and soils,

$$\boldsymbol{P}_f = \boldsymbol{M}_f\ddot{\boldsymbol{X}}_f + \boldsymbol{C}_f\dot{\boldsymbol{X}}_f + \boldsymbol{K}_f\boldsymbol{X}_f \tag{1}$$

in which $\mathbf{P}_f$ represents interaction-force vector, and $\mathbf{X}_f$ denotes the generalized displacement vector (such as translational displacements $\mathbf{u}_f$ for sway vibration or rotation angles θ_f for rocking motion), $\mathbf{M}_f$, $\mathbf{C}_f$ and $\mathbf{K}_f$ are mass, damping and stiffness matrices for foundation system, which are 2*2 symmetric matrices in the forms of

$$\boldsymbol{M}_f = M_{fe}\begin{bmatrix} m^*_{f1} & 0 \\ 0 & m^*_{f2} \end{bmatrix} \quad \boldsymbol{C}_f = C_{fe}\begin{bmatrix} c^*_{f1}+c^*_{f2} & -c^*_{f2} \\ -c^*_{f2} & c^*_{f2}+c^*_{f3} \end{bmatrix} \tag{2a}$$

$$\boldsymbol{K}_f = K_{fe}\begin{bmatrix} k^*_{f1}+k^*_{f2} & -k^*_{f2} \\ -k^*_{f2} & k^*_{f2}+k^*_{f3} \end{bmatrix} \tag{2b}$$

where the elements inside the matrix symbol are normalized coefficients, which are listed in Table 1 for four typical values of Poisson's ratio ν, and

$$M^r_{fe} = \frac{8\rho r_0^3}{2-\nu}, \quad C^r_{fe} = \frac{8\rho V_s r_0^2}{2-\nu}, \quad K^r_{fe} = \frac{8\rho V_s^2 r_0}{2-\nu} \tag{3a}$$

for horizontal vibration and

$$M^r_{fe} = \frac{8\rho r_0^5}{2-\nu}, \quad C^r_{fe} = \frac{8\rho V_s r_0^4}{2-\nu}, \quad K^r_{fe} = \frac{8\rho V_s^2 r_0^3}{2-\nu} \tag{3b}$$

for rocking motion. And ρ, V_s and ν are respectively mass density, shear-wave velocity and Poisson's ratio of subsoils, r_0 is the equivalent radius of footing disc.

VIBRATION EQUATIONS OF SOIL-STRUCTURE INTERACTION SYSTEM

Suppose that the typical superstructure is represented by a n-story shear-type structure as shown in Fig.4. In this MDOF modelling, the lump mass of the j-th layer is m_j, the mass inertial moment is J_j, total initial lateral stiffness and viscous damping coefficient of the layer members are k_j and c_j, the total mass and inertial moment of the footing are m_b and J_b. The total lateral displacement of the j-th mass can be written as,

$$u^t_{sj} = u_{sj} + (u_{f1} + \theta_{f1}H_j) + (u_g + \theta_g H_j) \tag{4}$$

in which u_g and θ_g are horizontal and rocking components of ground motions; u_{f1} and θ_{f1} are horizontal displacement and rotation of footing; H_j is the height is the j-th floor from the ground surface; u_{sj} is the displacement of the j-th lump mass relative to footing. The independent unknowns of the interaction system include the relative displacements of superstructure and horizontal displacements $\mathbf{u}_f=[u_{f1}\ u_{f2}]^T$ as well as rotation angles $\theta_f=[\theta_{f1}\ \ \theta_{f2}]^T$ of the additional oscillators for reproducing soil impedances. Referring to Eq.4, the global dynamic equilibrium equations of the superstructure can be formed,

$$\boldsymbol{M}_s\ddot{\boldsymbol{U}}_s + \boldsymbol{M}_s\boldsymbol{I}_n\ddot{u}_{f1} + \boldsymbol{M}_s\boldsymbol{H}\ddot{\theta}_{f1} + \boldsymbol{C}_s\dot{\boldsymbol{U}}_s + \boldsymbol{K}_s\boldsymbol{U}_s = -\boldsymbol{M}_s\boldsymbol{I}_n\ddot{u}_g - \boldsymbol{M}_s\boldsymbol{H}\ddot{\theta}_g \tag{5}$$

in which $\mathbf{M}_s$, $\mathbf{C}_s$ and $\mathbf{K}_s$ are global mass, damping and stiffness matrices of the superstructure. Usually, damping matrix $\mathbf{C}_s$ can be formed by Rayleigh proportional-damping concept (Luan 1992). And $\boldsymbol{I}_n=[1\ 1\ \ldots\ 1]^T$ and $\mathbf{H}=[H_1\ H_2\ \ldots\ H_n]^T$ are column vectors with n-order. The equation of sway motion of the coupled structure and footing system supported on soil media can be obtained by adding the total inertial forces induced in the structure and footing and the horizontal interaction force of soils,

$$(\boldsymbol{M}_s\boldsymbol{I}_n)^T\ddot{\boldsymbol{u}}^t_s + (m_b + m^h_{f1})(\ddot{u}_{f1} + \ddot{u}_g) + \boldsymbol{K}^h_{f1}\boldsymbol{u}_f + \boldsymbol{C}^h_{f1}\dot{\boldsymbol{u}}_f = 0 \tag{6a}$$

where $\mathbf{K}_{f1}{}^h$, and $\mathbf{C}_{f1}{}^h$ are the first row vector of the matrices $\mathbf{K}_f{}^h$ and $\mathbf{C}_f{}^h$ in Eq.2 with the superscript h denoting horizontal vibration mode. For the second additional block in the discrete model of soil impedances, the equation of motion can be similarly established as following,

$$m^h_{f2}(\ddot{u}_{f2} + \ddot{u}_g) + \boldsymbol{C}^h_{f2}\dot{\boldsymbol{u}}_f + \boldsymbol{K}^h_{f2}\boldsymbol{u}_f = 0 \tag{6b}$$

Combining these two formulae yields the governing equations of horizontal vibrations of the footing-foundation system. The corresponding equations for rocking motion can be got in a similar manner. The resulting equations of motion of the interaction system with (n+4) DOFs can be finally written in the following compacted form,

$$\boldsymbol{M}\ddot{\boldsymbol{u}} + \boldsymbol{C}\dot{\boldsymbol{u}} + \boldsymbol{K}\boldsymbol{u} = \boldsymbol{F} \tag{7}$$

in which $\mathbf{M}$, $\mathbf{C}$ and $\mathbf{K}$ are the global property matrices, $\mathbf{u}$ is the global displacement vector and $\mathbf{F}$ is the total load vector of the system,

$$\boldsymbol{M} = \begin{bmatrix} \boldsymbol{M}_s & \boldsymbol{M}^h_{sf} & \boldsymbol{M}^r_{sf} \\ \boldsymbol{M}^h_{fs} & \boldsymbol{M}^h_f & \boldsymbol{M}^{hr}_f \\ \boldsymbol{M}^r_{fs} & \boldsymbol{M}^{rh}_f & \boldsymbol{M}^r_f \end{bmatrix}, \quad \boldsymbol{C} = \begin{bmatrix} \boldsymbol{C}_s & \boldsymbol{C}^h_{sf} & 0 \\ \boldsymbol{C}^h_{fs} & \boldsymbol{C}^h_f & 0 \\ 0 & 0 & \boldsymbol{C}^r_f \end{bmatrix}, \quad \boldsymbol{K} = \begin{bmatrix} \boldsymbol{K}_s & \boldsymbol{K}^h_{fs} & 0 \\ \boldsymbol{K}^h_{fs} & \boldsymbol{K}^h_f & 0 \\ 0 & 0 & \boldsymbol{K}^r_f \end{bmatrix} \tag{8a}$$

$$\boldsymbol{u} = [\boldsymbol{u}_s\ \boldsymbol{u}_f\ \boldsymbol{\theta}_f]^T, \qquad \boldsymbol{F} = [\boldsymbol{F}_s\ \boldsymbol{F}^h_f\ \boldsymbol{F}^r_f]^T \tag{8b}$$

in which

$$\boldsymbol{M}^h_{fs} = (\boldsymbol{M}^h_{sf})^T = [\boldsymbol{M}_s\boldsymbol{I}_n\ 0\ 0]^T, \quad \boldsymbol{M}^r_{fs} = (\boldsymbol{M}^r_{sf})^T = [\boldsymbol{M}_s\boldsymbol{H}\ 0\ 0]^T \tag{9}$$

$$\boldsymbol{M}^h_f = \begin{bmatrix} M^h_{f1} & \\ & m^h_{f2} \end{bmatrix}, \quad \boldsymbol{M}^r_f = \begin{bmatrix} M^r_{f1} & \\ & m^r_{f2} \end{bmatrix}, \quad \boldsymbol{M}^{hr}_f = \boldsymbol{M}^{rh}_f = \begin{bmatrix} M_1 & \\ & 0 \end{bmatrix} \tag{10}$$

where

$$M^h_{f1} = M_0 + m_b + m^h_{f1}, \quad M^r_{f1} = M_2 + J_b + \sum_{j=1}^{n} J_j + m^r_{f1} \tag{11a}$$

$$M_0 = \sum_{j=1}^{n} m_j, \quad M_1 = \sum_{j=1}^{n} m_j H_j, \quad M_2 = \sum_{j=1}^{n} m_j H_j^2 \tag{11b}$$

$$\boldsymbol{F}_s = -\boldsymbol{M}_s\boldsymbol{I}_n\ddot{u}_g - \boldsymbol{M}_s\boldsymbol{H}\ddot{\theta}_g \tag{12a}$$

$$\boldsymbol{F}^h_f = -\boldsymbol{M}^h_f\boldsymbol{I}_2\ddot{u}_g - \boldsymbol{M}^{hr}_f\boldsymbol{I}_2\ddot{\theta}_g, \quad \boldsymbol{F}^r_f = -\boldsymbol{M}^{rh}_f\boldsymbol{I}_2\ddot{u}_g - \boldsymbol{M}^r_f\boldsymbol{I}_2\ddot{\theta}_g \tag{12b}$$

in which $\mathbf{I}_2=[1\ 1]^T$.

NONLINEAR HYSTERETIC RESTORING-FORCE MODEL

Structural members exhibit pronounced nonlinear hysteretic behavior under strong earthquake motion. The analytical models for backbone restoring-force characteristics can be usually achieved by idealizing the experimentally-observed force-deflection curves for the basic structural elements. In fact, the multi-segments models and Ramberg-Osgood relation, as shown in Fig.5(a), are popularly applied in conventional studies. The trace of tips of all hysteresis

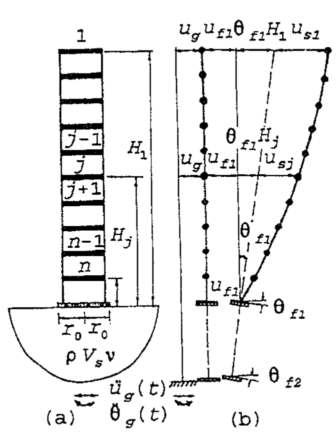

Fig.4. Computational Model of Soil-Structure Interaction Analysis

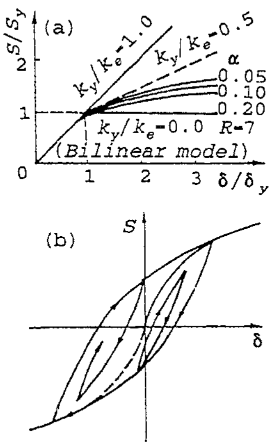

Fig.5. Nonlinear Model and Hysteretic Curve

loops, associated with different levels of cyclic deformation, is defined as the skeleton curve for structural elements. This curve constitutes the basis for characterizing the dynamic restoring force-deflection behavior for nonlinear analysis. For example, the relations between the layer shear force S and relative displacement δ for Ramberg-Osgood model can be expressed as

$$\delta/\delta_y = S/S_y[1+\alpha(S/S_y)^{R-1}] \tag{13}$$

where δ_y and S_y are respectively yield deflection and yield shear strength with the relation of $S_y=k_e\delta_y$, and k_e is the initial stiffness, α and R are respectively model parameters for defining shape and size of skeleton curve and hysteresis loops in the Ramberg-Osgood model. The various nonlinear characteristics from the linear elastic model to the elasto-perfectly-plastic model can be simulated by changing the values of parameters α and R, as illustrated in Fig.5(a).

Based on the backbone curve of structural member under virgin loading condition, Masing's rules are currently the most widely-applied criteria for constructing the unloading or reloading branch curves. Under the regularly periodic loading pattern, these loading and unloading rules contain two items as stated by Jennings (1964) and Luan (1992). Actually, the earthquake-induced loading is not only rather fluctuate rapidly in magnitude but also alternate quite irregularly in direction. Therefore the simple Masing's rules must be extended to handle this type of randomly irregular loading patterns in a rational way. To furnish such simulations, the supplementary criteria proposed by Luan (1992) are utilized. Referring to Fig.5(b), the main additional revisions include: (1) The subsequent loading will follow the skeleton curve once the current unloading or reloading branch curve meets the initial curve; (2) The unloading or reloading path will go after these previously-memorized hysteresis curves if the current loading reaches the maximum or minimum branch curves or/and the latest positive half cycle or negative half cycle attained in the past loading process. In order to strictly implement these criteria in the numerical simulation, the important issue is how to make an exact judgement for possible loading branch curve and rationally predict the up-date states of force and deformation based on the current force-deflection history. It is shown on the basis of numerous test computations that not only the state and corresponding loading curve at the last loading step must be memorized, but also the two reversal points corresponding to two loading branches as well as two bound half-cycle hysteresis curves attained in the previous history respectively in the positive and negative directions are required to be stored in the memory (Luan 1992).

TIME-DOMAIN NUMERICAL ITERATIVE PROCEDURE

When the above-illustrated structural nonlinear hysteretic behaviour is introduced in the equations of motion of soil-structure interaction system, Eq.7 must be solved by a certain step-by-step scheme in the time-domain because of the nonlinear dependency of stiffness matrix of structure on the deformation. As an integral, $\mathbf{K}_s(\mathbf{u}_s,\dot{\mathbf{u}}_s)\mathbf{u}_s$ represents the resulting nodal force vector caused by the resultant restoring forces in each story. For such nonlinear problems, the incremental-iterative algorithm with constant-stiffness formulation proposed by Luan (1992) is employed herein, in which the step-by-step time integration procedure for dynamic situation is combined with the load transfer approach for nonlinear analysis. In the incremental form of Eq.7, the resulting right-hand force vector contains two terms arising from nonlinear effects, i.e., (1) The equivalent nodal forces which are in equilibrium with the true restoring forces of structural member at the previous time step, and (2) Incremental unbalanced forces due to the deviation between elasto-plastic solution and linear elastic approximation of restoring forces for the iteration. These should be carefully established according to the above-illustrated restoring-force model and loading criteria. More details can be found elsewhere (Luan 1992).

NUMERICAL COMPUTATIONS WITH DISCUSSIONS

Three typical multi-layer shear-type structures, i.e., (1) S1: a 8-DOFs frame (Luan 1992), (2) S2: a nuclear power plant containment shell modelled with 8 lumped masses and (3) S3: a ten-floor building (Ghaffar-Zadeh and Chapel 1983), are analyzed by the proposed method. Their structural parameters together with the properties of underlying half-space soil are listed in Tables 2-4 respectively.

TABLE 2.Characteristics Parameters of S1

	1	2	3	4	5	6	7	8
m(t)	450	450	450	450	450	450	600	400
k_e(10^5kN/m)	1.00	1.00	1.40	1.40	1.60	1.60	1.80	2.00
δ_y(cm)	0.90	0.90	1.00	1.00	1.05	1.05	1.10	1.15
H(m)	25.6	22.4	19.2	16.0	12.8	9.60	6.40	3.20

Note: m_b=5212t, J_b=46904t·m^2; r_0=12m; ρ=1.78t/m^3, ν=1/3.

TABLE 3.Characteristics Parameters of S2

	1	2	3	4	5	6	7	8
m(t)	1825	3650	3650	3650	3650	3650	3650	3650
k_e(10^4kN/m)	137	137	137	137	137	137	137	137
δ_y(cm)	0.10	0.10	0.10	0.10	0.10	0.10	0.10	0.10
H(m)	61.8	54.3	46.8	39.3	31.8	24.3	16.8	9.25
J(10^3t·m^2)	342	684	684	684	684	684	684	684

Note: m_b=12500t, J_b=1267000t·m^2; r_0=20m; ρ=1.6t/m^3, ν=1/3.

TABLE 4. Characteristics Parameters of S3

	1	2	3	4	5	6	7	8	9	10
m(t)	1000	1500	1500	1500	1500	1500	1500	1500	1500	1500
k_e(10^4kN/m)	1.00	1.00	1.00	1.50	1.50	1.50	3.00	3.00	3.00	4.50
δ_y(cm)	1.00	1.00	1.00	1.20	1.20	1.20	1.50	1.50	1.50	1.50
H(m)	36.0	32.4	28.8	25.2	21.6	18.0	14.4	10.8	7.20	3.60

Note: m_b=3140t, J_b=317000t·m²; r_0=20m; ρ=1.6t/m³, ν=1/3.

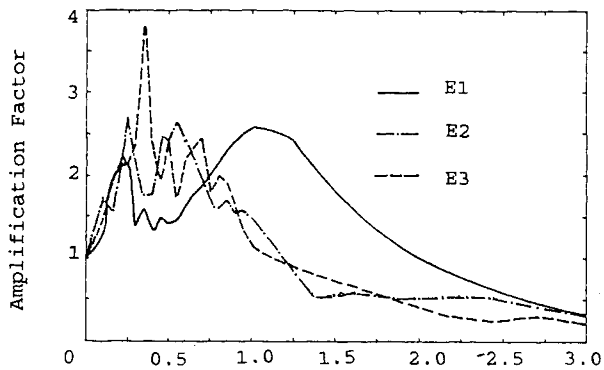

Fig.6. Acceleration Response Spectra of the Selected Ground Motions

Three representative earthquake records, i.e., (1) E1: the acceleration time history measured at the Tianjin Hospital during Tangshan Earthquake (1976) of China, (2) E2: the N-S horizontal acceleration component of El-Centro Earthquake and (3) E3: Taft Earthquake accelerogram, are selected as input ground motions at baserock or far-field. Their corresponding acceleration response spectra with the critical damping value of 5% are depicted in Fig.6. The predominant period of E1 which contains wide frequency components is over 1 Sec. E2 has rich components around 0.25-0.55 Sec, and Taft record (E3) has three peaks respectively at 0.35 Sec, 0.5 Sec and 0.7 Sec.

Comparative studies for numerical results are conducted to examine the effects of underlying soil shear stiffness and different ground motions on both vibration characteristics and dynamic responses of these three structures. The first four natural periods of these three structures with use of the initial stiffnesses founded on rigid base or on flexible subsoils are calculated from Eq.7. The computational results are delineated in Fig.7. With the decrease of the soil shear velocity, the natural periods of the coupled soil-structure interaction systems get longer. Moreover, the soil-structure interaction has more notable influence on vibration behaviour of stiff structures than on that of flexible structures.

In the nonlinear analyses, the representative values of α and R are respectively taken as 0.4 and 7 in the restoring-force model of structural members. The maximum displacement and acceleration responses at the top of the structure S1 as well as the maximum shear forces and relative deflections at the 6-th layer member are given in Fig.8 which display as complex functions of shear stiffness of foundation soils and input ground motions. The soil-structure interaction effect strongly depends on the characteristics of ground motions at the far field. The same structure subjected to different earthquake excitations may experience rather different stress and deformation behaviour. When subjected to the E1-type ground motion, the structure S1 founded on soft subsoils may undergo heavy seismic response both in displacements and accelerations and in shear forces and lateral deflections within structural members with respect to supported on rigid base. However, under the excitation of El Centro acceleration (E2), with the decrease of the shear modulus of underlying soils, the seismic responses of the same structure are considerably reduced. In addition, while this structure S1 is shaken by Taft Earthquake, neither very soft foundations nor rather solid subsoils result in the largest seismic responses in the super-structure. The foundation soils with a certain high shear rigidity, which cause the fundamental period of coupling system to approach to the predominant period of the ground motion, initiate fair high structural seismic responses.

At the same time, the above conclusions can be substantiated by the comparisons in Table 5. Under the same ground motions, different structures may undergo different seismic responses. For the flexible structures, soil-structure interaction effect is of minor significance in most cases, which can be negligible in the standpoint of engineering practices. For the structures with high stiffnesses, soil-structures interaction effect cannot be overlooked especially when the natural frequency of the coupling system is near the predominant frequency of the ground motion.

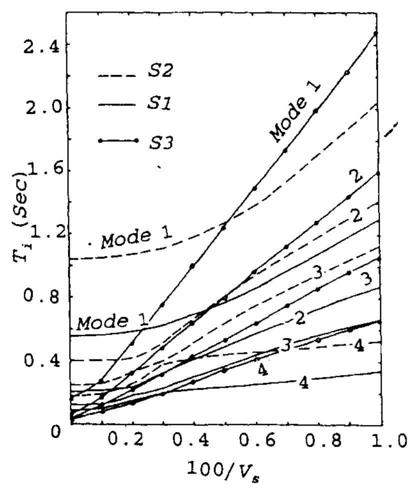

Fig.7. Effects of Soil Shear Stiffness on Structural Vibration Characteristics

CONCLUDING REMARKS

In this paper, a simplified mechanical model with 8 lumped parameters for simulating dynamic impedance functions is proposed and then applied in the time-domain dynamic analysis of the nonlinear soil-structure interaction system. Because of the frequency-independent nature of the lumped parameters, this model is expected to

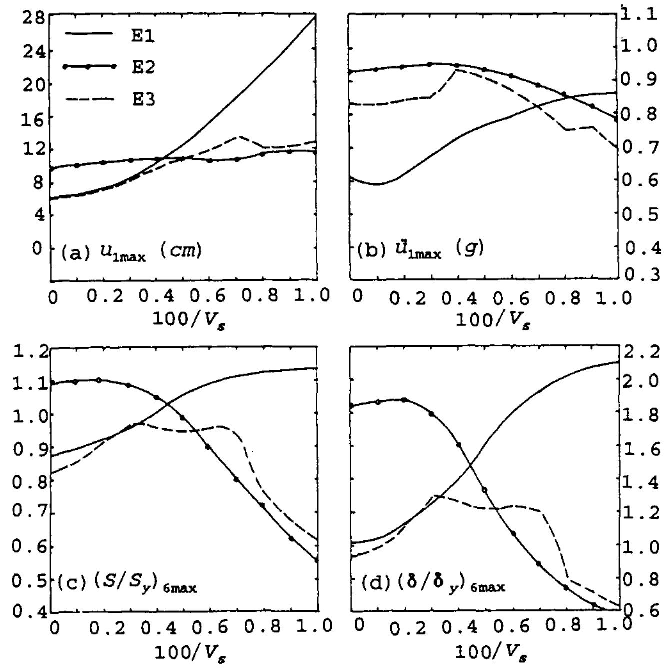

Fig.9. Effects of Soil Shear Stiffness on Structural Seismic Responses

TABLE 5. Maximum Seismic Responses of Three Structures Subjected to Different Input Ground Motions

	V_s (m/s)	S1 E1	S1 E2	S1 E3	S2 E1	S2 E2	S2 E3	S3 E1	S3 E2	S3 E3
u_{1max} (cm)	100	27.7	11.5	12.9	51.2	28.6	20.9	41.5	13.2	18.3
	200	12.5	10.8	10.8	31.2	12.8	13.8	37.1	11.6	16.1
	400	7.8	10.6	7.9	5.6	8.9	5.8	35.9	11.6	15.0
	∞	6.2	9.7	6.0	0.5	0.6	0.8	35.4	11.1	14.5
$\ddot{u}_{1max}$ (g)	100	0.86	0.78	0.69	0.65	0.28	0.31	0.48	0.41	0.42
	200	0.77	0.94	0.91	1.02	0.53	0.57	0.45	0.46	0.49
	400	0.64	0.95	0.85	0.63	1.14	0.86	0.44	0.44	0.54
	∞	0.61	0.93	0.84	0.75	0.89	0.87	0.45	0.49	0.55
$(S/S_y)_{6max}$	100	1.13	0.56	0.62	0.35	0.25	0.15	1.47	0.89	1.05
	200	1.05	0.98	0.95	1.03	0.42	0.43	0.95	1.02	1.23
	400	0.94	1.10	0.94	0.80	1.09	0.73	0.93	1.11	1.27
	∞	0.88	1.10	0.83	0.83	0.89	0.96	0.91	1.18	1.29
$(\delta/\delta_y)_{6max}$	100	2.09	0.57	0.63	0.35	0.25	0.15	7.26	1.07	1.60
	200	1.62	1.34	1.22	1.50	0.42	0.43	1.21	1.46	2.94
	400	1.20	1.86	1.19	0.87	1.81	0.77	1.18	1.96	3.42
	∞	1.03	1.85	0.94	0.93	1.06	1.25	1.13	2.43	3.67

be potentially useful in the time-domain analysis for complex nonlinear structures. The equations of motion of the coupling system are formulated by the step-by-step time-domain scheme. The comparative analyses for the representative structures have shown that the soil-structure interaction will have appreciable influences on stiff structures, especially subjected to the ground motion of which predominant period approaches to the natural period of the coupled superstructure-footing-foundation system. Furthermore, seismic response behavior of nonlinear structures is intimately associated with the characteristics of earthquake shaking.

ACKNOWLEDGEMENTS

The financial support by the National Natural Science Foundation of China through the Grant NSF59109071 is gratefully acknowledged.

REFERENCES

De Barros, F.C.P. and J.E. Luco (1990), "Discrete Models for Vertical Vibrations of Surface and Embedded Foundations", Earthquake Engineering and Structural Dynamics, 19:289-303.

Gazetas, G. (1983), "Analysis of Machine Foundation Vibrations: State of the Art", Soil Dynamics and Earthquake Engineering, 2(1):2-42.

Ghaffar-Zadeh, M. and F. Chapel (1983), "Frequency-Independent Impedances of Soil-Structures Systems in Horizontal and Rocking Modes", Earthquake Engineering and Structural Dynamics, 11:523-540.

Jean, W.-Y., T.-W. Lin and J. Penzien (1990), "System Parameters of Soil Foundations for Time Domain Dynamic Analysis", Earthquake Engineering and Structural Dynamics, 19:541-553.

Jennings, P.C. (1964), "Periodic Response of a General Yielding Structures", Journal of the Engineering Mechanics Division, ASCE, 90(EM2):131-166.

Luan, M.-T. (1992), "An Effective Algorithm with Application for Dynamic Analysis of Shear-Type Nonlinear Systems", Nonlinear Vibration, Branching and Chaos, Tianjin University Press.

Veletsos, A.S. and Y.T. Wei (1971), "Lateral and Rocking Vibrations of Footings", Journal of the Soil Mechanics and Foundations Division, ASCE, 97(SM9):1227-1249.

Wolf, J.P. and D.R. Somaini (1986), "Approximate Dynamic Model of Embedded Foundation in Time Domain", Earthquake Engineering and Structural Dynamics, 14:683-703.